



# Overexpression of *PtPEPCK1* gene promotes nitrogen metabolism in poplar

Lina Wang<sup>1</sup> · Miao He<sup>1</sup> · Song Chen<sup>1</sup> · Kean Wang<sup>1</sup> · Donghai Cui<sup>1</sup> · Xin Huang<sup>2</sup> · Lijie Liu<sup>2</sup>

Received: 14 March 2017 / Accepted: 15 May 2018 / Published online: 8 October 2019  
© Northeast Forestry University 2019

**Abstract** To understand the function of phosphoenolpyruvate carboxylase kinase, we introduced *PtPEPCK1* gene under the control of 35S promoter into 84K poplar (*Populus alba* × *P. glandulosa*). *PtPEPCK1* gene is well-known for its role in gluconeogenesis. However, our data confirmed that it has significant effects on amino acid biosynthesis and nitrogen metabolism. Immunohistochemistry and fluorescence microscopy indicate that *PtPEPCK1* is specifically expressed in the cytoplasm of the spongy and palisade tissues. Overexpression of *PtPEPCK1* was characterized through transcriptomics and metabolomics. The metabolites concentration of the ornithine cycle and its precursors also increased, of which *N*-acetylornithine was up-regulated almost 50-fold and ornithine 33.7-fold. These were accompanied by a massive increase in levels of several amino

acids. Therefore, overexpression of *PtPEPCK1* increases amino acid levels with urea cycle disorder.

**Keywords** Amino acid metabolism · Metabolome · Nitrogen metabolism · Phosphoenolpyruvate carboxylase kinase · Transcriptome · Urea cycle

## Introduction

Phosphoenolpyruvate carboxylase kinase (PEPCK, EC 4.1.1.49) is a bifunctional enzyme and a key enzyme of metabolic pathways of plants (Huang et al. 2015). The roles of this enzyme in gluconeogenesis and anaplerotic reactions have been widely reported (Walker and Leegood 1996; Winger 1999). In C<sub>4</sub> and CAM plants, PEPCK acts as a decarboxylase and provides CO<sub>2</sub> for photosynthesis (Edwards et al. 1971). Several reports suggest that *PtPEPCK1* plays a key role in amino acid metabolism in C<sub>3</sub> plants (e.g. Lea et al. 2001; Martín et al. 2011). Recent researches indicate that PEPCK is involved in the conversion of the carbon skeleton of asparagine/aspartate (oxaloacetate) to glutamate/glutamine (Lea et al. 2001). In addition, the roles of PEPCK in amino acids and nitrogenous metabolism through regulating energy equilibria are outlined in several studies (Urbina et al. 1990; Murooka et al. 2002; Owen et al. 2002; Maciaga and Paszkowski 2004; Habash and Bernard 2009; Mattoo et al. 2015). Our experimental data confirmed that it has prominent effects on nitrogen metabolism in *Populus*, and the conclusions of this experiment are partly consistent with those of previous studies (Walker et al. 1999; Leegood and Walker. 2003; Famiani et al. 2018).

Phosphoenolpyruvate (PEP) and oxaloacetate (OAA) are key intermediates in gluconeogenesis and tricarboxylic acid (TCA) cycle. PEP is a precursor of aromatic amino acids and

Project funding: This work was supported by the grants from the National Natural Science Foundation of China (No. 3180030530), and the Fundamental Research Funds for the Central Universities (2572019BA14).

The online version is available at <http://www.springerlink.com>

Corresponding editor: Yanbo Hu.

**Electronic supplementary material** The online version of this article (<https://doi.org/10.1007/s11676-019-01042-4>) contains supplementary material, which is available to authorized users.

✉ Lina Wang  
wanglina@nefu.edu.cn

<sup>1</sup> State Key Laboratory of Tree Genetics and Breeding, Northeast Forestry University, 51 Hexing Road, Harbin 150040, People's Republic of China

<sup>2</sup> College of Life Sciences and Agriculture and Forestry, Qiqihar University, Qiqihar 161006, People's Republic of China

a phosphate donor in the phosphotransferase system. OAA is the precursor of amino acids derived from aspartate and intermediate in the TCA cycle. Amino acids are the hubs and centers associated with nitrogen assimilation and carbon metabolism. The amide group of asparagine is metabolized into ammonia, which is redistributed through the glutamate synthase cycle. The amino group of aspartic acid can be directly used in the synthesis of lysine, threonine, methionine or isoleucine (Azevedo et al. 1998); it can also be converted into  $\alpha$ -oxoglutaric acid to produce glutamic acid and oxaloacetate (Fig. 1a).

The role of PEPCK anaplerotic reactions in many organisms has been discussed extensively (Walker and Leegood 1996; Wingler 1999; Lea et al. 2001; Sun 2018). Both PEPCK and PEPCK can form a middle bridge between the oxaloacetate/aspartate family of amino acid, including lysine, threonine, asparagine, tyrosine, and tryptophan, which are synthesized via the shikimate pathway, and alanine derived from pyruvate (Famiani et al. 2018) (Fig. 1b).

During the development of grape seeds and pea, PEPCK expression was highest when amino acid reached its maximum before storage protein deposition (Walker et al. 1999). Delgado-Alvarado et al. (2010) suggested that PEPCK is involved in the nitrogen-containing solutes during the development of pea, and the proteins were strongly induced in vitro in the seed coat by nitrate ( $\text{NO}_3^-$ ), ammonium ( $\text{NH}_4^+$ ), and asparagine (Asn). When nitrogen or amine compounds were applied externally, PEPCK protein expression was more dramatically intense than that

of other enzymes (Walker et al. 1999; Chen et al. 2000). In seed coats, PEPCK protein was strongly enhanced by  $\text{NO}_3^-$  and  $\text{NH}_4^+$  (50-fold), and by Asn (25-fold), whereas was not influenced by urea, Glu, Gln, and Asp. In contrast,  $\text{NO}_3^-$ , ammonia, Glu, and Asn had much weaker effects on PEPCK. Exogenous application of Asn significantly increased the content of PEPCK protein (25 times), while other nitrogen compounds did not. PEPCK is also thought to play a role in the metabolism and the transport of nitrogenous compounds (Urbina et al. 1990; Walker et al. 1999; Chen et al. 2000; Owen et al. 2002; Walker and Chen 2002; Leegood and Walker 2003; Pinto et al. 2014).

Plants with  $\text{C}_4$  enzymes have advantages in extreme growing conditions and the  $\text{C}_4$  enzymes participate in the process of concentrating  $\text{CO}_2$  in  $\text{C}_4$  photosynthesis. However, the effect of phosphoenolpyruvate carboxykinase of  $\text{C}_4$  for  $\text{C}_3$  plants is unknown. From previous studies, PEPCK has also been reported to play a key role in amino acid metabolism and the conversion of the carbon skeleton, the backbone of carbon molecules. However, in spite of considerable research on PEPCK, the effects of *PtPEPCK1* on nitrogen flow has not been determined. In this study, we modulated the metabolic flow by overexpressing *PtPEPCK1* under the control of 35S promoter into *Populus*. Our results showed that overexpression of *PtPEPCK1* increases the content of amino acids, nitrogen metabolism with urea cycle disorder. The higher the level of *PtPEPCK1*, the greater the growth inhibition. This paper reveals the importance of *PtPEPCK1* in promoting nitrogen metabolism in  $\text{C}_3$  plants.

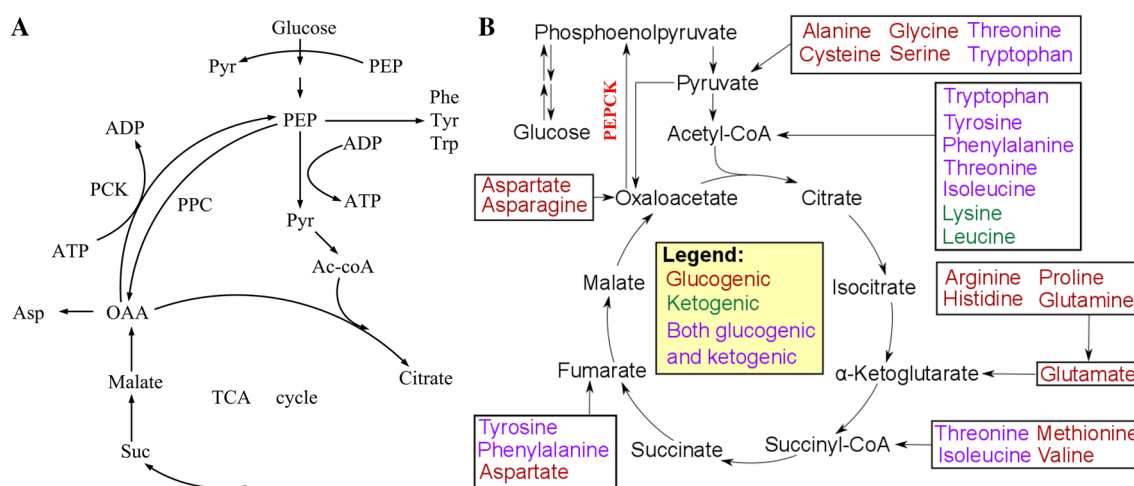


**Fig. 1** **a** Schematic diagram of the relationship between PEP and OAA metabolism modulated by phosphoenolpyruvate carboxykinase. Abbreviations: AcCoA: acetyl coenzyme A; Asp: aspartate; Phe: phenylalanine; Pyr: pyruvate; Trp: tryptophan; Tyr: tyrosine; Suc:

succinate; TCA: tricarboxylic acid (Chao and Liao 1994); **b** pathways involved in the synthesis and metabolism of glycine, alanine, serine, cysteine, aspartic acid, asparagine, glutamic acid, glutamine, proline and ornithine (Wang 2011)

## Materials and methods

### Plant materials

Explants for gene transformation were prepared from seedlings of 84K poplar (*Populus alba* × *P. glandulosa*) which were acquired from the State Key Laboratory of Tree Genetics and Breeding of the Northeast Forestry University in Harbin, Heilongjiang.

All non-transgenic and transgenic plants were 25-day old and grown in a growth chamber at  $25 \pm 2$  °C under a 16-h light/8-h dark photoperiod at a light intensity of 1000–1500 flux. Six *PtPEPCK1*-overexpressed transgenic lines (B5-M1, B5-M3, B5-M7, B5-M9, B5-A1, and B5-A2), and three non-transgenic plants (wild-type) (WT1, WT2, and WT3) were used for RNA-seq and metabolome analysis.

### Vector construction, transformation, and regeneration

The coding sequence of *PtPEPCK1* was cloned into the Gateway entry vector pENTR/SD/D-TOPO. LR reactions were performed to clone DNA fragments into donor vectors according to the manufacturer's instructions. The polymerase chain reaction (PCR) cycle was initial denaturation at 95 °C for 3 min followed by 32 cycles of 30 s denaturation at 95 °C, 30 s of annealing at 58 °C and 1 min of extension at 72 °C. PCR products were separated by electrophoresis on a 1.2% agarose gel. This entry plasmid was used to generate *pGWB5-PtPEPCK1* by introducing the *PtPEPCK1* gene to the constructed vectors. The PCR fragment was directly cloned into the entry vector pENT/TOPO and transferred into the Gateway *pGWB5* vector using the Gateway LR Clonase enzyme. Details of the two methods of transformation with modifications from previous research (Confalonieri et al. 1994) are shown in supplementary experimental procedures.

### RNA extraction and cDNA synthesis

Total RNA was extracted using a plant RNA extraction kit (Tiangen Co., Beijing, China). One microgram (µg) of total RNA was treated with DNase I. The integrity of the purified RNA was assessed by Agilent 2100 Bioanalyzer and agarose gel electrophoresis.

First-strand cDNA was synthesized with a Reverse transcriptase MMLV Kit (Invitrogen) using Oligo (dT)-primers. The volume of reverse transcription reaction was 20 µL, and the cDNA was used as the template for semi-quantitative RT-PCR, performed with a pair of primers specific to the *PtPEPCK1* gene (*PtPEPCK1*-F: 5'-ATGGACAACAAGGCACCTGACAAT-3'; *PtPEPCK1*-R: 5'-GTAATTAGGACCAGCTGCCAGAATC-3'). The annealing temperature

for RT-PCR was 58 °C and with 35 reaction cycles. The amplified DNA products were separated on 2.0% (w/v) agarose gel.

### Molecular analysis (RT-PCR and qRT-PCR analysis)

Real-time PCR was performed on an optical 96-well plate with an Yena real-time PCR system using the primer pairs 5'-GCTCAGGGTGCTTTCAATGCTATCT-3' (forward primer) and 5'-TGTGGAGGTAATGGGTAAACTTGAG-3' (reverse primer) for *PtPEPCK1* and 5'-AAACAATGGCTGATGCTG-3' (forward primer) and 5'-ACAATACCGTGTCAATAGG-3' (reverse primer) for actin. The temperatures profile was (1) 95 °C for 10 min, 40 cycles of 95 °C for 15 s, and 60 °C for 1 min and (2) melt curve analysis with measurements between 60 and 95 °C. The  $\Delta\Delta C_t$  method was used in calculations. For each sample, three independent qPCR experiments were performed. Each experiment involved three replicates for each line. We averaged  $C_q$  data from three independent experiments to derive mean  $C_q$  values and  $C_q$  standard deviation.

### Western blotting

Total protein of poplar leaves was extracted by TCA-acetone precipitation. The 2-D Q method was used for protein quantification; 40 µg of protein were separated on 10% SDS-PAGE electrophoresis and transferred to PVDF membrane. The membranes were then blocked with 3% BSA in PBS for 2 h and incubated with the monoclonal antibody (Institute of Plant Research, Chinese Academy of Sciences, Beijing) overnight at 4 °C. After washing in PBS, the membranes were incubated with horseradish peroxidase (HRP)-conjugated secondary antibody for 1 h at room temperature. Antibody-antigen complexes were then detected using an ECL chemiluminescent detection system (Biyuntian Co., Beijing, China).  $\beta$ -actin was used as a loading control. All treatments were done in triplicate.

### Library construction, sequencing, and assembly

The mRNA libraries were sequenced based on the protocol of the Illumina RNA-seq Library Preparation Kit for Transcriptome analysis. Fifteen cDNA libraries, named as non-transgenic, *PtPEPCK1*-overexpressed transgenic lines, were sequenced on an Illumina HiSeq2000. The specific process is shown in supplementary experimental procedures 2. After sequencing, the raw sequence data were first purified by trimming adapter sequences and removing low-quality sequences. The resulting clean reads were de novo assembled and mapped to the transcriptome.

## Functional annotation and differentially expressed unigene (DEU) analysis

Unigenes were functionally annotated by performing BLAST searches with an E-value  $< 1 \times 10^{-5}$  against NCBI non-redundant, and Swiss-Prot, Kyoto Encyclopedia of Genes and Genomes (KEGG), and Clusters of Orthologous (COG) protein databases. The proteins with the highest similarities were retrieved for analysis. Incongruent results from different databases were settled under a priority order of NCBI, Swiss-Prot, KEGG (Jiang et al. 2016). Based on their Nr annotations, all unigenes were assigned Gene Ontology annotations using BLAST2GO followed by functional classifications using WEGO software (Li et al. 2017). In addition, presumed metabolic pathways were assigned to each unigene by performing BLASTx searches against the KEGG pathway database with an E-value threshold of  $1 \times 10^{-5}$ . Gene expression levels were normalized using the reads per kilobase per million mapped reads (RPKM) method. DEUs were identified by pairwise comparison of transgenic and NT lines using the edgeR package (Felice et al. 2013). DEU significance was based on a false discovery rate of 0.1% and an absolute log2 fold change of 1. Fisher's exact test was used to determine the significance of DEU-mapped GO terms and pathways.

## Gene expression characterization using metabolomics

Chemicals and materials used for solvent preparation: HPLC-grade methanol (Merck Co., Kenilworth, Illinois, USA) and chloroform (Burdick & Jackson Co., city, state, USA), ultrapure water (Bedford, Massachusetts, USA), 98% formic acid (Kyungkido Co., Suwon, Korea), and HPLC-grade ammonium acetate (Tedia, Fairfield, Connecticut, USA). Used to standardize the signal intensity: an internal standard solution containing 10 mM L-methionine sulfones (Sigma Co., Saint Louis, Missouri, USA) and D-camphor-10-sulfonic acid sodium salt (Sigma Co., Saint Louis, Missouri, USA) in methanol (Internal Standard Solution 1, ISS1). Used to adjust the migration time: one mM 3-amino-pyrrolidine dihydrochloride (Sigma Co., Saint Louis, Missouri, USA), *N,N*-diethyl-2-phenylacetamide (Sigma Co., Saint Louis, Missouri, USA), trimesic acid (Sigma Co., Saint Louis, Missouri, USA) and disodium 3-hydroxynaphthalene-2, 7-disulfonate (Sigma Co., Saint Louis, Missouri, USA) in water (Internal Standard Solution 2, ISS2).

CE-MS sample preparation: The 70-mg transgenic poplar samples were accurately weighed in 2 ml EP tubes and then added with 700  $\mu$ L precooled 10  $\mu$ M ISS1 (Internal Standard Solution 1, ISS1). Precision weighing Berberine HCL Standard 5.0 mg to 50 mL capacity bottle, dissolved with methanol and diluted to scale, the configuration of internal standard reserve liquid, diluted with methanol, that is ISS1

working fluid. 1 mM 3-amino-pyrrolidine, *N,N*-diphenylacetamide, pyromellitic acid, and 2-naphthol-3,6-Disulfonic acid were used as internal standard 2 to correct migration time drift during the operation of capillary electrophoresis. Vortex the mixture thoroughly for 30 s, then add 700  $\mu$ L extractant chloroform, vortex again for 30 s, then add 250  $\mu$ L Milli-Q water, and then vortex for 30 s. Place the mixture at 4 °C for 10 min, then centrifuge at 4 °C at 9100g for 10 min, collect 500  $\mu$ L supernatant, and centrifuge at 4 °C at 12,000g for about 2 h. The sample was filtered through a microporous 5-kDa ultrafilter tube (5 kDa) (Japanese HMT), for 10 min. The filtrate was lyophilized (4–6 h), and the lyophilized sample was redissolved with an aqueous solution containing 50  $\mu$ M internal standard 2 (Internal Standard Solution 2, ISS2), which was resuscitated for CE-MS detection.

CE-TOF/MS Analysis: Tissue metabolomics profiling was performed on a CE (G7100A, Agilent, Santa Clara, CA)—TOF/MS (G6224A, Agilent) system equipped with an ESI-MS sprayer kit (G1607A, Agilent), a 1260 ISO pump (G1310B, Agilent) and a mini chiller (Huber, Germany). The separation was performed using a bare capillary column (id. 50  $\mu$ m  $\times$  80 cm) and maintained at 20 °C (Yu 2012). The capillary was rinsed with the electrolyte solution for 1 h at the first use. The capillary column and sample cell temperatures were 5 °C. The 50% aqueous solution of the sheath liquid contained 6-(2,2-trifluoromethoxy) phosphazene at a concentration of 0.1  $\mu$ M as a reference ion of the corrected mass. The sheath fluid flow rate was 10  $\mu$ L min<sup>-1</sup> and the split ratio was 1:100. In positive ion mode, the background electrolyte is a 4% aqueous formic acid solution, and the electrolyte is replaced every 10 pins to ensure the repeatability and stability of the analysis. The injection was 50 m bar for 10 s, the separation voltage was 27 kV, and the separation time was 30 min. CE-TOF/MS analysis of the tissue samples was carried out in both the cation-positive (CP) model and the anion-negative (AN) (Zhao 2016). The parameters of these two modes were described by Zeng et al. (2013).

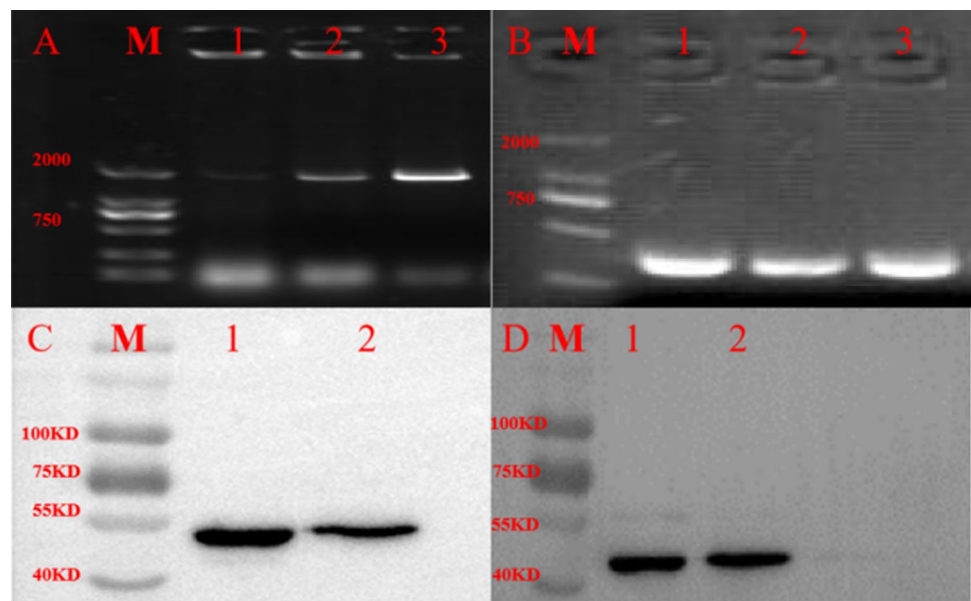
## Results

### Tissue-specific expression and *Agrobacterium*-mediated transformation

In this study, RT-PCR and western blotting were used for tissue-specific expression analysis of the *PtPEPCK1* gene. RT-PCR results showed significant differences in mRNA expression of *PtPEPCK1* in different tissues, with the highest expression level in poplar leaves (Fig. 2a, b). The results of western blotting showed that the expression of *PtPEPCK1* protein was detected in the leaves and stems but not in the roots (Fig. 2c, d).



**Fig. 2** RT-PCR and western blotting were used for tissue-specific expression analysis of the *PtPEPCK1* gene; **a** agarose gel electrophoresis of PCR products of the *PtPEPCK1* gene in roots (A1), stems (A2) and leaves (A3); **b** agarose gel electrophoresis of PCR products of the reference gene actin in the roots (B1), stems (B2) and leaves (B3); **c** western blotting for tissue-specific expression analysis of the *PtPEPCK1* gene in leaves (C1), stems (C2); **d** detection of the expression level of actin protein in leaves (D1) and stems (D2)



To characterize the function of *PtPEPCK1* gene in *Populus*, overexpression vectors were constructed under the control of the cauliflower mosaic virus 35S promoter. *Agrobacterium tumefaciens* GV3101, harboring the binary plasmid *pGWB5*, was employed according to Nakagawa et al. (2007). The recombinant vector was transferred into *Agrobacterium tumefaciens* incubated with leaf discs for callus induction and shoot regeneration (dark-induction method) and direct adventitious bud differentiation regeneration (light-induced method). Dark- and light-induced systems are the two protocols developed for successful regeneration of poplar and their protocols are described in detail in the Supplemental experimental procedure 1 (Confalonieri et al. 1994; Movahedi et al. 2014). These protocols will serve as powerful tools for studies of the developmental processes in poplar. An overview of the steps used in the *Agrobacterium tumefaciens* transformation of *Populus* is presented in Fig. 3. A combination of the two methods can help maximize efficiency and high levels of gene expression in transgenic plants. This provides a useful foundation for further research toward the development of 84K poplar (Wang et al. 2017).

### Molecular analysis of *PtPEPCK1* in transgenic plants

To verify whether the *PtPEPCK1* gene had been integrated into the poplar genome and expressed, expressions of *PtPEPCK1* at the transcriptional and protein levels in the rooted plantlets were also confirmed in each transgenic line by RT-PCR (Fig. 4a–d), western blotting assays (Fig. 4e–h). RT-PCR analysis used specific primers, *GFP* and *PtPEPCK1*; the *PtPEPCK1*-overexpressing lines displayed a band at 720 bp corresponding to the *GFP* gene and 2001 bp corresponding to the *PtPEPCK1* gene (Fig. 4a–c).

Using the *GFP* primers, the results showed that there was one band of the right size in each lane of transgenic plants, while there was no amplification product in the lane of wild-type and negative controls (Fig. 4c). Using the *PtPEPCK1* primers, the results showed that one strong band of the right size in each lane of transgenic plants, while there was a weak amplification product in the lane of the wild-type plant (Fig. 4).

### Subcellular localization of *PtPEPCK1*-GFP

Studies of protein subcellular localization are helpful in understanding the functions of proteins in plants. The use of green fluorescent protein (GFP) as a fusion tag has dramatically extended knowledge in this field. Stable transformation of GFP-tagged proteins has been widely used to study protein localization in vivo in different systems. In this study, IHC-P and fluorescence microscopy were used to locate *PtPEPCK1* expression. The results show that the cytoplasm of palisade and spongy tissues in leaves had strong positive expression characteristics: brownish or brownish yellow, bright and easy to see, and pale yellow granules in wild-type plants. Moreover, the expression of *PtPEPCK1* in mesophyll sponge tissue was higher than in palisade tissue (Fig. 5).

### Transcriptomes and metabolomes analysis

RNA-Seq experiments were performed with overexpressed and wild-type lines. Library sequencing and assembly were carried out as described in the Supplemental experimental procedure 2. The 28S, 18S and 5.8S bands of total RNA by agarose gel electrophoresis are shown in Fig. 6a. The bands were further assessed by Agilent 2100 Bioanalyzer (Fig. 6b).

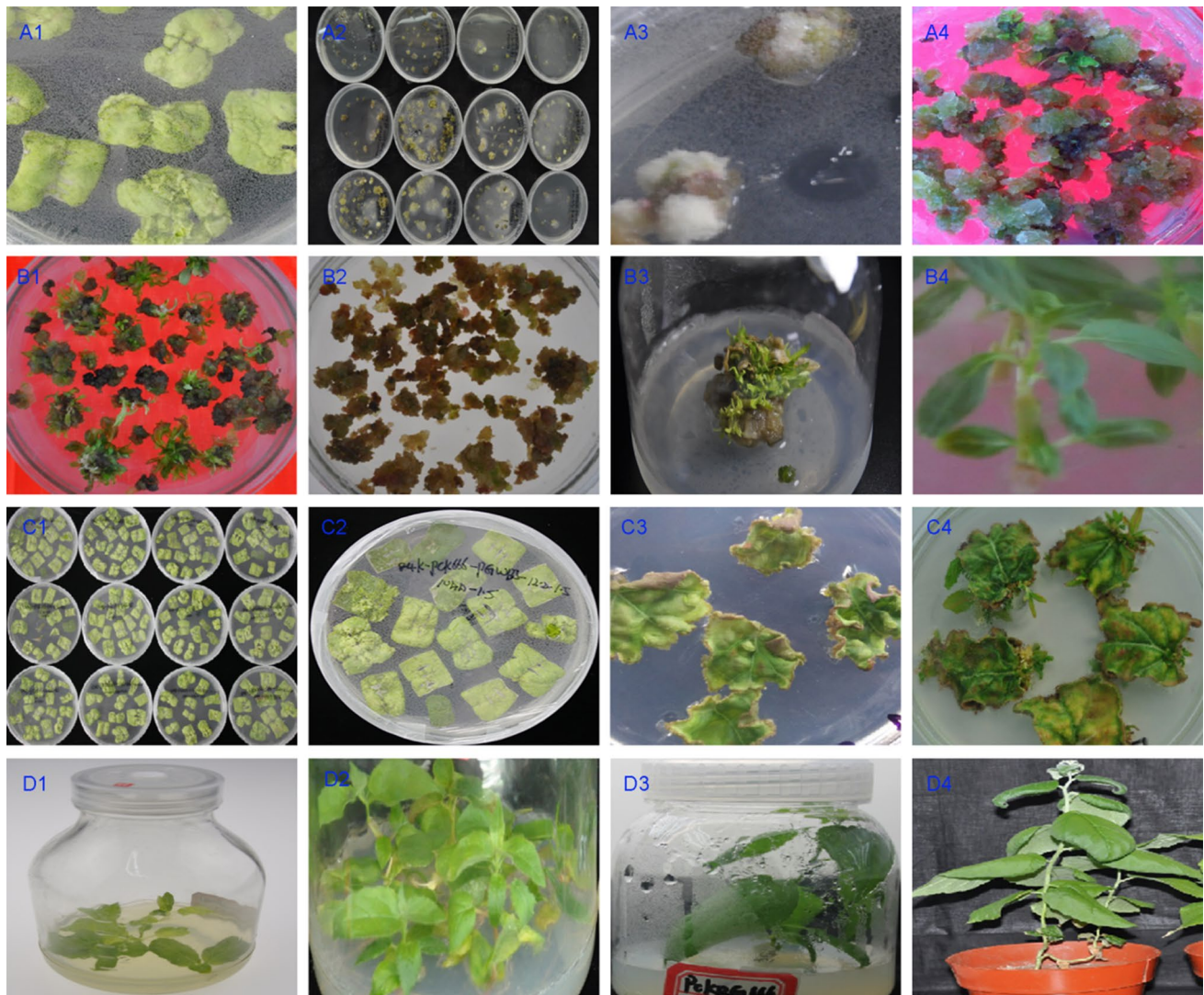


**Fig. 3** Regeneration of *Agrobacterium*-mediated transformed *Populus* by the dark-induced and light-induced methods; **A1** co-cultivation of leaf discs with *Agrobacterium* on MS medium in the dark; **A2–B2** callus induction in 84K poplar from leaves cultured on MS medium treated with various concentrations and combinations of 2,4-D, KT, and TDZ hormones after 8–10 weeks at  $25 \pm 2$  °C under dark conditions; **B3–B4** shoot regeneration from well-developed callus from different media; **B3** elongated shoots from clusters which had attained 2–3 cm in length; **B4** elongation period: transgenic plantlets forming roots within 2 weeks in kanamycin-containing rooting medium and

acclimatization period; **C1** and **C2** co-cultivation of leaf discs with *Agrobacterium* on MS medium in light and leaf explants cultured on selected media with 50 mg·L<sup>-1</sup> kanamycin and 300 mg·L<sup>-1</sup> cefotaxime for 3–4 weeks after co-cultivation; **C3** regenerated transformants on MS medium; **C4** regenerated transformants on MS medium generated with the optimization of transformation efficiency; kana-resistant shoots were further elongated in the medium and buds started appearing in clusters; **D1–D2** regeneration of plantlets in MS medium; **D3** transgenic plantlets forming roots within 2 weeks in rooting medium containing kanamycin; **D4** acclimatization period

The 18S-region and 28S-region cover the 18S peak and 28S peak, respectively. The 5S-region covers the small rRNA fragments (5S and 5.8S rRNA, and tRNA). The fast-region lies between the 5S-region and the 18S-region. The inter-region lies between the 18S-region and the 28S-region. And finally, the post-region lies beyond the 28S-region. The results of the detection transcriptome libraries are shown in Fig. 6c and Supplemental Table S1. As a result of sequencing, 773088030 reads were obtained using an Illumina Hiseq

platform (Supplemental Table S2). Quality assessment of the sequencing data using the Illumina guidelines showed that more than 92% of each sample had a quality score of Q30 (those with a base quality greater than 30). The RNA-Seq data in this study was sent to the National Center for Biotechnology Information (NCBI) (accession number: SRP112714). Using a statistical cutoff of  $< 0.005$  for the false discovery rate (FDR) and a fold change cutoff of  $> 2$  or  $< -2$ , we identified 4876 genes that were differentially



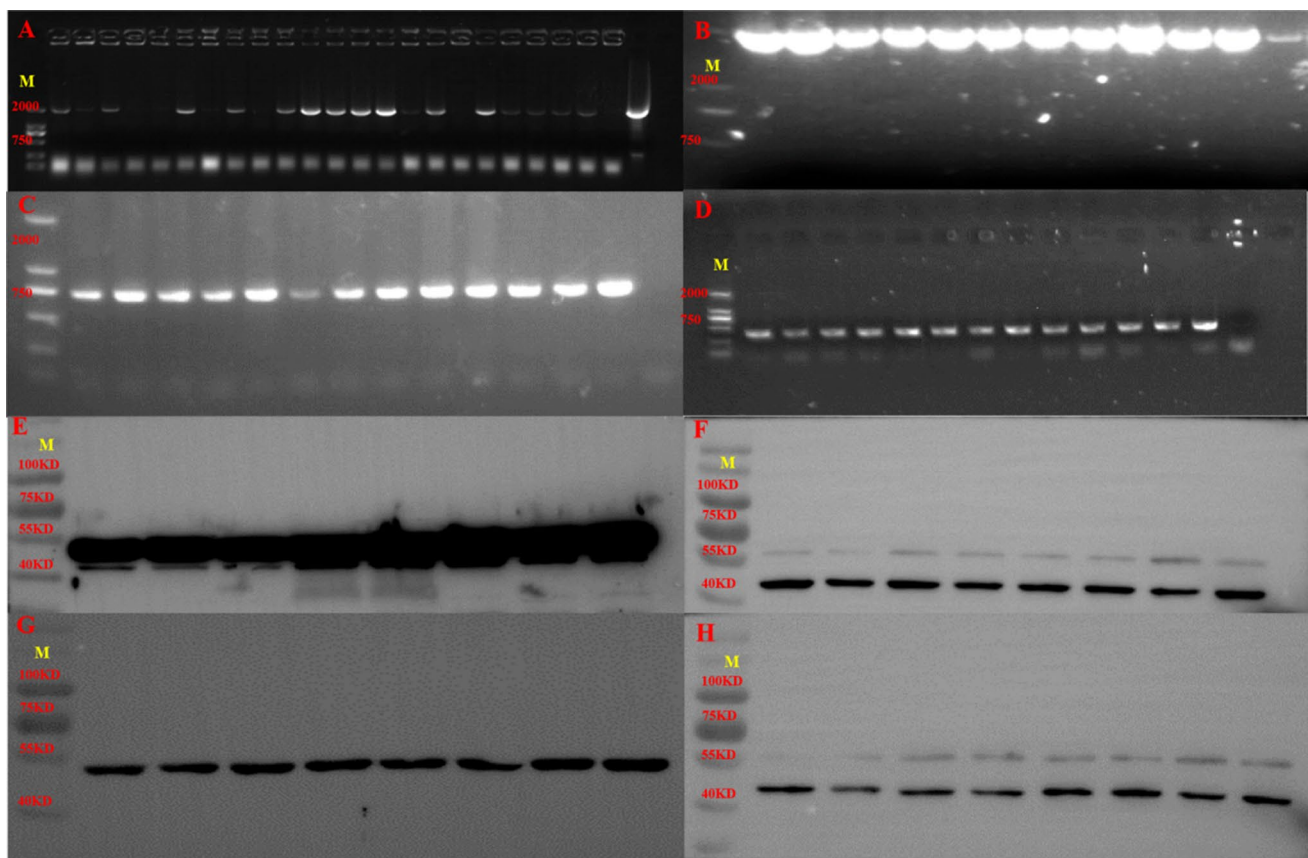


**Fig. 4** Molecular and biochemical characterization of transgenic plants. **a, b** RT-PCR analysis of overexpressing lines and wild-type lines using *PtPEPCK1* primers; a band in 2001 bp was observed. **c** RT-PCR analysis of the overexpressing lines and the wild-type lines using GFP primers. A band at 750 bp was observed in the overexpressing lines. **d** RT-PCR analysis of the overexpressing lines and the wild-type lines using NPTII primers. A band at 230 bp was

observed in the overexpressing lines. **e–h** The analysis of *PtPEPCK1* protein abundance in transgenic lines and wild-type by western blot analysis using anti-*PtPEPCK1* antibody. **e** The expression pattern of *PtPEPCK1* in overexpressing lines. **f** The expression pattern of β-actin in overexpressing lines. **g** The expression pattern of *PtPEPCK1* in wild-type. **h** The expression pattern of β-actin in wild-type

expressed in lines that overexpressed *PtPEPCK1* compared to controls. Among these, 3447 were upregulated and 1429 were downregulated. Hierarchical cluster analysis of differentially expressed genes and functional categorization of significant differentially expressed genes are shown in Fig. 6d. Pathway analysis of differential metabolites are shown in Fig. 6e. From the results, core nitrogen metabolic pathways were directly disturbed in transgenic lines.

#### Overexpression of *PtPEPCK1* increased amino acid metabolism

A number of major amino acids such as Gln, Asn, Gly, and Glu were all in higher amounts in the transgenic *PtPEPCK1* plants compared with the wild-types (Fig. 7). Amino acids are the main forms of nitrogen in plants and hence are major nitrogen carriers. The transcriptome data showed that alterations of 10 amino acid synthases were observed in overexpressed plants, eight of which were up-regulated and two

down-regulated. Detailed information on the up-regulation and down-regulation of amino acids is shown in Table 1.

The metabolomics analysis results were consistent with those from the amino acid biosynthesis data of transcriptome (Fig. 8 and Table 2), which showed the up-regulation of nine amino acids and down-regulation of four. When *PtPEPCK1* was overexpressed, increased amino acids were: Gln, 5.5 fold, Arg, 2.2-fold, Asn, 3.6-fold, Asp, 1.5-fold, Ser, 4.2-fold, Met, 2.4-fold, Pro, 2.4-fold, citrulline, 10.6-fold, and leu, 1.1-fold. Several amino acids decreased, Phe, 0.7-fold, Trp, 0.8-fold, Tyr, 0.6-fold, and L-isoleucine, 0.8-fold.

#### Urea cycle disorder (UCD) for ammonia detoxification and anaplerosis

The urea cycle (Fig. 9a) controls the removal of ammonia and is of central importance in plants, but the regulation of gene expression is poorly understood. Several recent studies (Roosens et al. 2002) have implicated, ornithine, a

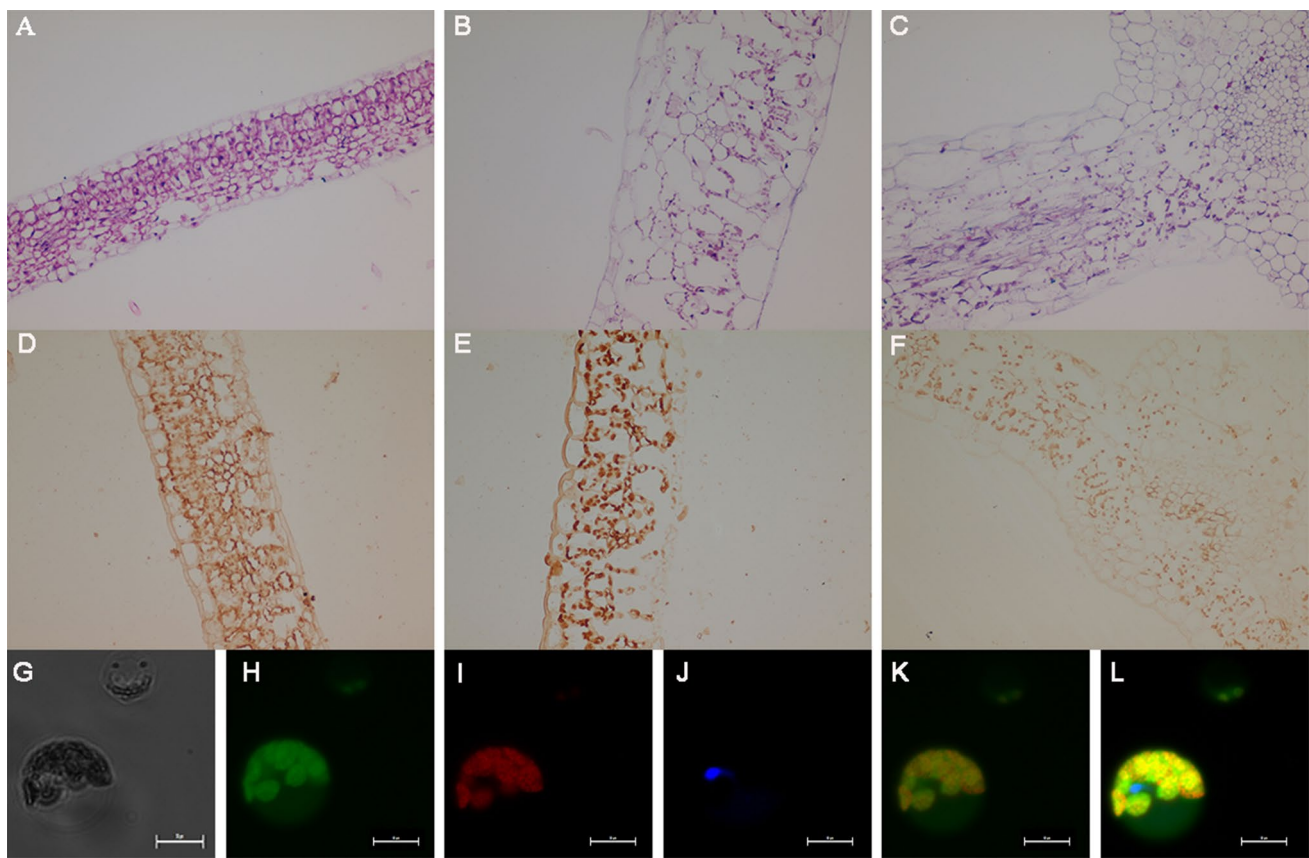


**Fig. 5** Subcellular localization of PtPEPCK1 in *Populus*. **a–c** HE sections and **d–f** IHC sections. **a, d** Transgenic line of *PtPEPCK1-PGWB5-M1*. **B, e** Transgenic line of *PtPEPCK1-PGWB5-M6*. **C, f** Wild-type. **g–l** Transgenic lines expression GFP with different localizations were tested for their emissions of fluorescence using ZEISS Axio Imager 2 Research Upright Micro-

scope. **g** Bright-field. **h** Green fluorescent protein (GFP). **i** Chlorophyll autofluorescence (Auto). **j** DAPI-stained nuclei were observed with a fluorescence microscope and DAPI served as a positive marker for nuclear localization. **k, l** Merged images. The 35S::GFP fusion was used as the positive protein control, and was detected in the cytoplasm of 84K poplar (**g–l**: Scale bar = 50 μm)

non-proteinogenic amino acid, as a regulator for the biosynthesis of several amino acids and PAs, including its own biosynthesis and accumulation. Urea is the end product of nitrogen metabolism, which takes place mainly in mitochondria and cytoplasm, and is the main pathway for ammonia disposal. The urea cycle, which consists of a series of five biochemical reactions, and carries five enzymes. The cycle is also maintained by other components such as the enzyme *N*-acetyl glutamate synthase (NAGS) that produces a positive regulator of CPS1 and two amino acid transporters, ornithine translocase and citrin. In plants, ornithine is synthesized mostly from glutamine, and the first enzyme believed to regulate the entire pathway is *N*-acetyl-Glu synthase (NAGS; EC 2.3.1.1). *N*-acetyl-Glu kinase (NAGK; EC 2.7.2.8) then converts acetyl-Glu into *N*-acetyl-Glu-5-phosphate which, via the intermediates *N*-acetyl-Glu-5-semialdehyde and *N*<sup>2</sup>-acetyl-Orn, is converted into ornithine which can be synthesized from arginine via arginase, the by-product being urea.

When compared to the wild-type, the *PtPEPCK1* transgenic seedlings had up to a 49.9-fold higher concentration of *N*-Acetyl-Orn, 33.7-fold of ornithine, and 20.0-fold of *N*-acetyl glutamate (Fig. 9 and Table 3). The transcription levels of urea, *N*-acetyl-Orn, and ornithine change significantly in transgenic plants. Urea is the end product of amino acid metabolism. The nitrogen from amino acids converted to ammonia is toxic to plants, and to prevent the accumulation of toxic nitrogenous compounds, the urea cycle incorporates unused nitrogen for net biosynthetic purposes into urea.

Phosphoenolpyruvate (PEP) and oxaloacetate (OAA) are key intermediates at the junction between catabolism and biosynthesis, occupying a central position. The flux between PEP and OAA can, therefore, be modulated by *PtPEPCK1*. To achieve manipulation of metabolic pathways by *PtPEPCK1*, it is essential to understand how the flux distribution can be altered by key genes and how the plants respond to metabolic perturbations introduced by genetic manipulations (Fig. 10).



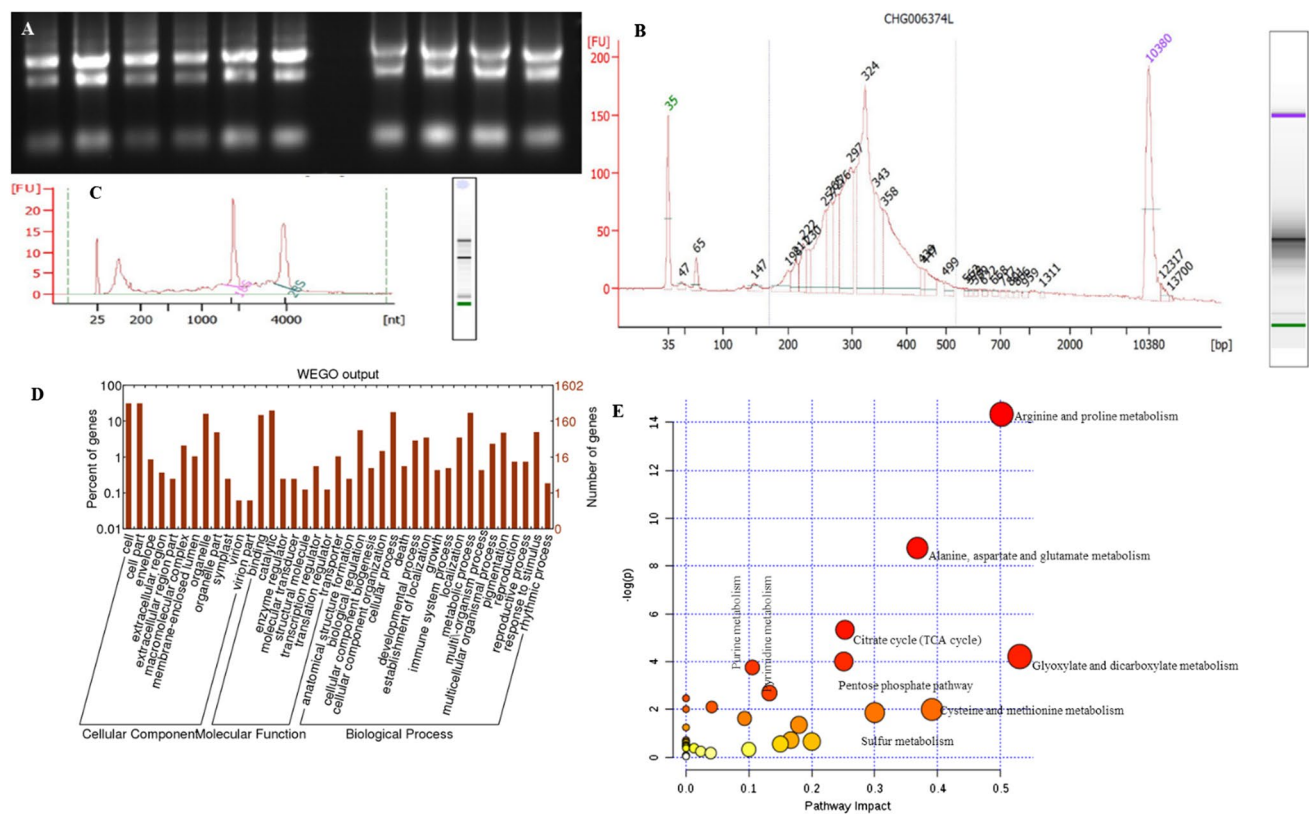


**Fig. 6** Results of transcriptomes and metabolomes analysis. **a** Agarose gel electrophoresis of total RNA. **b** Total RNA extracted from 84K poplar leaves, quality and quantity assessment using Agilent 2100 Bioanalyzer; **c** analysis of the transcriptome libraries prepared using mRNA obtained by the second purification strategy; **d** functional categorization of significantly differentially expressed genes in

the transgene. The results were summarized in three main categories: cellular component, molecular function, and biological process. The right Y-axis indicates the number of genes in each category. The left Y-axis indicates the percentages of a specific category of genes in that main category. **e** Pathway analysis of differential metabolites between WT and OE groups

Transgenic plants had disadvantageous conditions caused by overexpressed *PtPEPCK1* and developed strategies to adapt their metabolism which had been adversely affected, in order to survive under these conditions. The over-expression of *PtPEPCK1* seriously affected the core metabolism pathway, which included carbon flow to oxaloacetate, acetyl-CoA,  $\alpha$ -oxoglutarate, and pyruvic acid, all of which were precursors of amino acids.

## Discussion

What role does *PtPEPCK1* play in amino acid metabolism, amine metabolism and nitrogen metabolism in  $C_3$  plants? Early research found that the overexpression of *PEPCK* caused amino acid metabolism but was not involved in the urea cycle (Shi et al. 2015). Ornithine sits at the crossroads of interconversions of glutamate and arginine on the one hand, and the production of proline, polyamines (PAs) and

some alkaloids on the other (Majumdar et al. 2015). It is synthesized primarily from glutamine and as it is an intermediate metabolite of the PA and the amino acid biosynthetic pathways rather than a terminal product, the biosynthesis of ornithine is likely to be regulated by its increased demand for the production of Put, arginine or proline. Arginine and ornithine metabolism are of central importance in biology but the regulation of gene expression and the enzymes of the glutamine/ornithine/arginine biosynthesis are poorly understood.

Several mutants with altered amino acid concentrations have been reported. The overexpression of *Glutamine Dumper1* (*GDU1*) and its homologs results in a large increase in amino acids, especially of glutamine (Pilot et al. 2004). Overexpression of the *noduline-93* gene (*OsENOD93-1*), which contains two transmembrane domains and is localized to mitochondria, increases xylem amino acid levels. In either case, the exact mechanism is not completely understood (Price et al. 2013). Overexpression of the

## BIOSYNTHESIS OF AMINO ACIDS

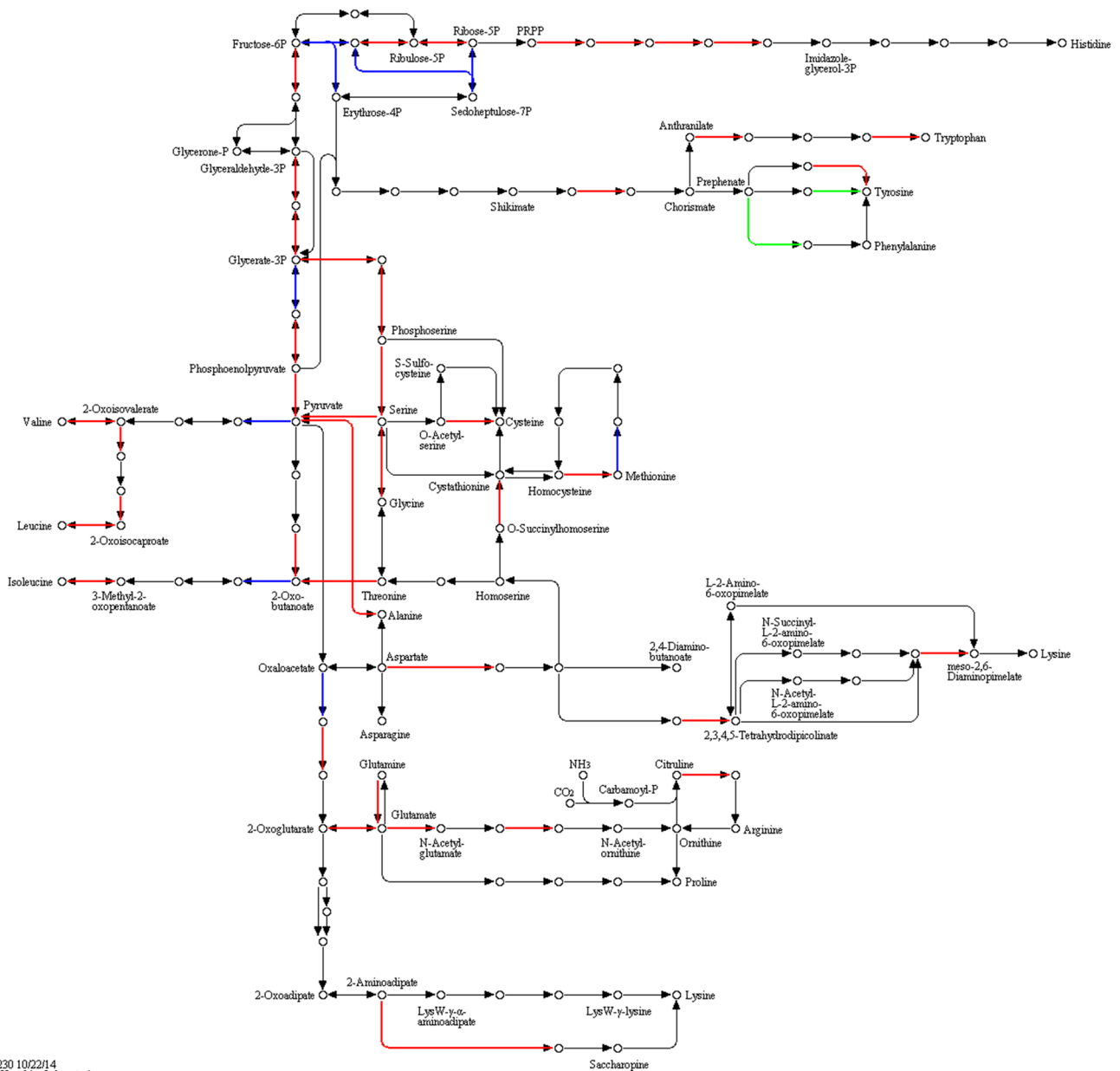


**Fig. 7** Comparative analysis of gene enrichment of amino acid metabolism induced by transgenic *PtPEPCK1* gene at the transcription level. The amino acid biosynthesis pathway was taken from KEGG at <http://www.genome.ad.jp/kegg/>. Note: Red shows upregulation, green shows downregulation, blue indicates that the gene has two or more transcripts, and annotation information is both upregu-

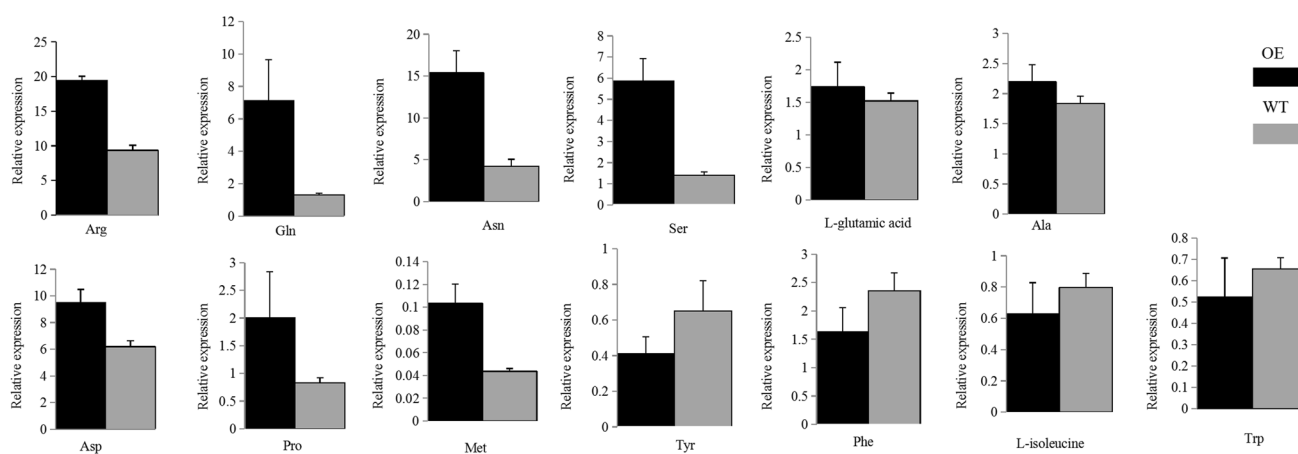
lated and downregulated. The amino acids increased significantly as alanine, glutamine, and L-proline. The amino acids that did not increase significantly were: L-serine, L-glutamic acid, aspartic acid, and methionine. Amino acids that decreased significantly were L-isoleucine, tryptophan, phenylalanine, and tyrosine

*PtPEPCK1* gene in this study is similar to previous studies and promotes nitrogen metabolism. The metabolites significantly increased in the transgenic lines were *N*-acetylornithine (49.9-fold), ornithine (33.7-fold), citrulline (10.6-fold),

argininosuccinic acid (8.2-fold), arginine (2.1-fold), and urea (5.7-fold). These were accompanied by a massive increase in several amino acids including glycine, alanine, leucine, proline, serine, methionine, asparagine, aspartic acid,

**Table 1** Transcripts of amino acid synthase and their changes in overexpressing *PtPEPCK1* plants

Name	Definition of Enzyme	Entry	ko_ID
Glutamate-glyoxylate aminotransferase (GGAT)	[EC:2.6.1.4 2.6.1.44]	K14272	c1_g2_i32261 (3.643938723) c1_g2_i4544 (1.45711666)
Glutamate synthase (NADH)	[EC:1.4.1.14]	K00264	c1_g2_i30364 (2.379670256)
Argininosuccinate synthase (argG, ASS1)	[EC:6.3.4.5]	K01940	c1_g2_i11366 (2.261077437)
Aspartate kinase (lysC)	[EC:2.7.2.4]	K00928	c1_g2_i55843 (1.520301952)
Amino-acid <i>N</i> -acetyltransferase(argAB)	[EC:2.3.1.1]	K14682	c1_g2_i24986 (3.616045198)
<i>N</i> -acetyl-gamma-glutamyl-phosphate reductase(argC)	[EC:1.2.1.38]	K00145	c1_g2_i53833 (4.9117545)
4-Hydroxy-tetrahydrodipicolinate reductase (dapB)	[EC:1.17.1.8]	K00215	c1_g2_i15724 (1.002505443)
S-adenosylmethionine synthetase (metK)	[EC:2.5.1.6]	K00789	c1_g2_i33099 (2.390264162) c1_g2_i42158 (− 1.451291831)
Arogenate/prephenate dehydratase (ADT, PDT)	[EC:4.2.1.91 4.2.1.51]	K05359	c1_g2_i31324 (− 1.15417688)
Tyrosine aminotransferase (TAT)	[EC:2.6.1.5]	K00815	c1_g2_i17192 (− 1.438409444)

**Fig. 8** The amino acid content of the overexpressed *PtPEPCK1* gene was changed, among which 13 amino acids were changed, 9 were up-regulated and 4 were down-regulated**Table 2** Different metabolites of amino acids, modified amino acids, and small peptides

Name	Mean OE	Mean WT	SE-OE	SE-WT
Gln	7.1184	1.3005	2.5353	0.1101
Asn	15.3758	4.2366	2.6596	0.8196
Ser	5.8661	1.4071	1.0617	0.1472
Met	0.1036	0.0435	0.0168	0.0025
Ala	2.1958	1.8375	0.2849	0.1196
Asp	9.5112	6.1940	0.9750	0.4467
Pro	2.0066	0.8272	0.8317	0.0909
Arg	19.3984	9.3553	0.6345	0.7297
L-Glutamic acid	1.7375	1.5222	0.3786	0.1187
Phe	1.6291	2.3572	1.6291	0.3113
L-Isoleucinesn	0.6271	0.7983	0.2009	0.0878
Trp	0.5234	0.6556	0.1825	0.0518
Tyr	0.4111	0.6508	0.0952	0.1697

glutamate, arginine, and especially of glutamine. Detailed analysis of the transcriptome and metabolome, the total number of metabolites present, of the transgenic plants, indicates that *PtPEPCK1* is involved in amino acid and nitrogen metabolism.

Research has shown that the transfer of *PEPCK* has a negative regulation of plant growth (Huang et al. 2015). In the *PEPCK*-deficient lines, prominent growth suppression of newly germinated tomato seedlings was observed. The phenotypic analyses of the 35S pro: SIPEPCK RNAi lines showed that systemic suppression of *PEPCK* reduced the growth of the seedlings. In the *PEPCK*-deficient lines, prominent growth suppression of germinated seedlings was observed and other vegetative suppression appeared during the early stages of growth in the 35S promoter-driven lines. In tomato fruit, suppression of *PEPCK* expression by RNA interference driven by a fruit ripening-specific promoter



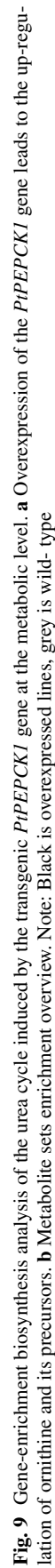


**Table 3** Comparative analysis of changes in the levels of urea cycle between transgenic lines and wild-type

Name	Mean OE	Mean WT	SE-OE	SE-WT
N-Acetylglutamic acid	0.60176803	0.081509	0.175184	0.025809
N-Acetylornithine	1.09333447	0.02191	0.680769	0.000764
Arg	19.3984408	9.355363	0.634594	0.72979
Argininosuccinic acid	0.03758348	0.004583	0.010629	0.000343
Ornithine	5.64518819	0.167589	2.563472	0.027961
Cinulline	0.64105307	0.060567	0.423036	0.010287
Urea	19.2965009	3.364934	4.195495	0.267731

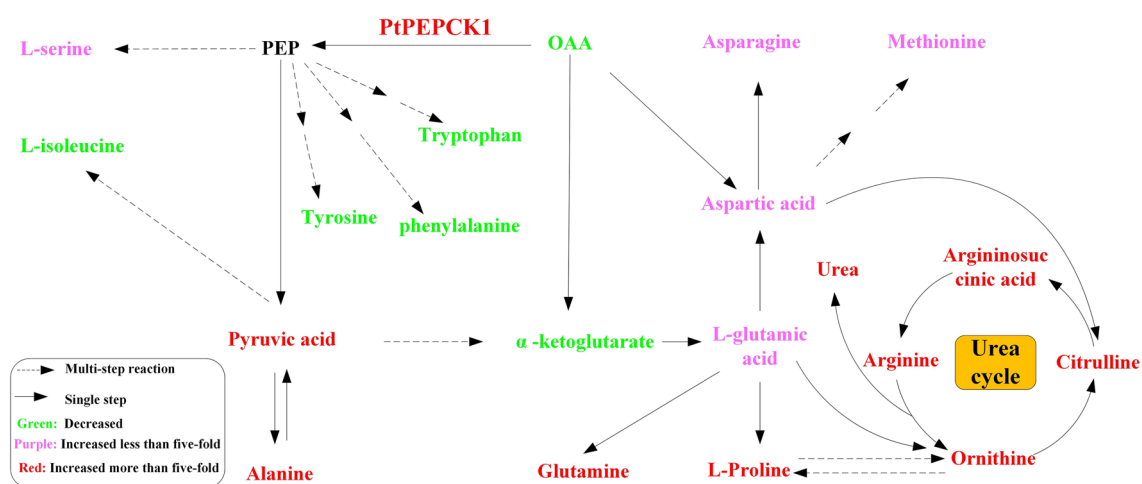
resulted in the accumulation of malate with a decrease in sugar contents (Osorio et al. 2013). It was also reported that there was a significant reduction of fructose and glucose accompanied by malate accumulation in ripening transgenic tomato in which PEPCK expression was suppressed. These results suggest that the major metabolic pathways of carbon and nitrogen were influenced by *PEPCK*. Not surprisingly, amino acid levels respond to a myriad of environmental stimuli, such as nitrogen stress (Balint and Rengel 2011), the light/dark cycle, mineral nutrition stress, and other abiotic stresses.

The regulation of metabolic flow is the key to determine the synthesis rate and yield of aromatic compounds (Liu et al. 2006). Furthermore, the biosynthesis of secondary metabolites such as flavonoids and phenylpropanoid were affected and the plant-pathogen interaction was influenced by the *PtPEPCK1* gene. Choi et al. (2015) suggested that *CaPEPCK* contributes positively to natural plant immunity against hemibiotrophic bacterial (Du et al. 2015). Studies of the roles of *PEPCK* in immune systems have been limited

to animals and bacteria. For example, Chen et al. (2002) reported evidence of PEPCK in plant defense-related structures such as trichomes, oil and resin ducts. However, the involvement of plant *PEPCK* in defense response remains unclear and *PEPCK* may be induced in plants by a series of biotic and abiotic stimuli.

Transgenic research has attracted considerable attention as a way to enhance and improve abiotic stress tolerance of plants (Hussain et al. 2011). Research in China and in other countries have used transgenic technology to over-regulate the expression of key enzymes in single carbon and nitrogen metabolism and its effect on biomass growth. However, many results were on the increase in expression of the target gene while biomass correspondingly decreased. In this study, the gene in carbon and nitrogen metabolism, *PtPEPCK1*, was transferred into  $C_3$  poplar seedlings for overexpression. The core metabolic pathway of the plants was seriously affected and there was strengthening or slowing down of localized carbon flow at the transcriptional level. The change of local carbon flow caused the imbalance of other metabolic pathways and imbalance within each (Hu et al. 2014), which is concealed by some concurrent mechanisms that maintain steady-state in plants.

Genetic Modification technology is used to express the key genes of carbon and nitrogen metabolism and its effect on biomass growth. However, many results show the increase of gene expression but biomass has not increased accordingly. In this study, overexpression of the *PtPEPCK1* gene did not achieve high photosynthetic efficiency. On the contrary, the growth rate of transgenic plants was lower than that of wild type plants. The effects of local carbon flow enhancement or inhibition on the growth of the plant population are not necessarily opposite. They are either alone or individually inhibiting the expression of a key carbon and

**Fig. 10** Summary of the changes and trends of amino acids and urea cycle in overexpressing *PtPEPCK1* plants. Note: red shows upregulation, green shows downregulation, and pink less than five times up-

regulated. Solid lines represent only one path, and dotted lines represent multiple paths

nitrogen metabolic gene, *PtPEPCK1*. The core metabolic pathway of the plants has been seriously affected and disrupted and changes in expression have been observed at the transcriptional level. However, regulation of the underlying mechanisms of photosynthesis, the formation of tissues, the coevolution of mesophyll cells and vascular bundle sheath cells can not alter in the C<sub>3</sub> plant carbon cycle.

## References

- Azevedo RA, Arruda P, Turner WL, Peter JL (1998) ChemInform abstract: biosynthesis and metabolism of the aspartate-derived amino acids in higher plants. *Cheminform* 29(2):395–419
- Bahrami AR, Chen ZH, Walker RP, Leegood R, Gray JE (2001) Ripening-related occurrence of phosphoenolpyruvate carboxykinase in tomato fruit[J]. *Plant Mol Biol* 47(4):499–506
- Balint T, Rengel Z (2011) Amino acid composition of xylem and phloem sap varies in canola genotypes differing in nitrogen- and sulfur-use efficiency. *Crop Pasture Sci* 62(3):198–207
- Chao YP, Liao JC (1994) Metabolic responses to substrate futile cycling in *Escherichia coli*. *J Biol Chem* 269(7):5122–5126
- Chen ZH, Walker RP, Acheson R, Técsi LI, Winkler A, Lea PJ, Leegood R (2000) Are isocitrate lyase and phosphoenolpyruvate carboxykinase involved in gluconeogenesis during senescence of barley leaves and cucumber cotyledons? *Plant Cell Physiol* 41(8):960–967
- Chen ZH, Walker RP, Acheson RM, Leegood RC (2002) Phosphoenolpyruvate carboxykinase assayed at physiological concentrations of metal ions has a high affinity for CO<sub>2</sub>. *Plant Physiol* 128(1):160–164
- Choi DS, Kim NH, Hwang BK (2015) The pepper phosphoenolpyruvate carboxykinase *capepck1* is involved in plant immunity against bacterial and oomycete pathogens. *Plant Mol Biol* 89(1–2):99–111
- Christian OB, Alexander S (2002) The malate dehydrogenase of *Ralstonia eutropha* and functionality of the C<sub>3</sub>/C<sub>4</sub> metabolism in a Tn5-induced *mdh* mutant. *FEMS Microbiol Lett* 212(2):159–164
- Confalonieri M, Balestrazzi A, Bisoffi S (1994) Genetic transformation of *Populus nigra* by *Agrobacterium tumefaciens*. *Plant Cell Rep* 13(5):256–261
- Delgado-Alvarado A, Walker RP, Leegood RC (2010) Phosphoenolpyruvate carboxykinase in developing pea seeds is associated with tissues involved in solute transport and is nitrogen-responsive. *Plant, Cell Environ* 30(2):225–235
- Du SC, Kim NH, Hwang BK (2015) The pepper phosphoenolpyruvate carboxykinase *CaPEPCK1* is involved in plant immunity against bacterial and oomycete pathogens. *Plant Mol Biol* 89(1–2):99–111
- Edwards GE, Kanai R, Black CC (1971) Phosphoenolpyruvate carboxykinase in leaves of certain plants which fix CO<sub>2</sub> by the C<sub>4</sub>-dicarboxylic acid cycle of photosynthesis. *Biochem Biophys Res Commun* 45(2):278–285
- Famiani F, Paoletti A, Proietti P, Battistelli A, Moscatello S (2018) The occurrence of phosphoenolpyruvate carboxykinase (PEPCK) in the pericarp of different grapevine genotypes and in grape leaves and developing seeds. *J Hortic Sci Biotechnol* 23:1–10
- Felice BD, Manfellotto F, Raffaella D, Olga DC, Antonietta DM, Marco T (2013) Comparative transcriptional analysis reveals differential gene expression between Sand Daffodil tissues. *Genetica* 141(10–12):443–452
- Habash DZ, Bernard SM (2009) The importance of cytosolic glutamine synthetase in nitrogen assimilation and recycling. *New Phytol* 182(3):608–620
- Hu YB, Bellaloui N, Sun GY, Tigabu M, Wang JH (2014) Exogenous sodium sulfide improves morphological and physiological responses of a hybrid *Populus* species to nitrogen dioxide. *J Plant Physiol* 171(10):868–875
- Huang YX, Yin YG, Sanuki A, Fukuda N, Ezura H, Matsukura C (2015) Phosphoenolpyruvate carboxykinase (PEPCK) deficiency affects the germination, growth and fruit sugar content in tomato (*Solanum lycopersicum* L.). *Plant Physiol Biochem* 96:417–425
- Hussain SS, Kayani MA, Amjad M (2011) Transcription factors as tools to engineer enhanced drought stress tolerance in plants. *Bio-technol Prog* 27(2):297–306
- Jiang F, Chen XP, Hu WS, Zheng SQ (2016) Identification of differentially expressed genes implicated in peel color (red and green) of *Dimocarpus confinis*. *SpringerPlus* 5(1):1088
- Lea PJ, Chen ZH, Leegood R, Walker RP (2001) Does phosphoenolpyruvate carboxykinase have a role in both amino acid and carbohydrate metabolism? *Amino Acids* 20(3):225–241
- Leegood RC, Ap RT (1978) Identification of the regulatory steps in gluconeogenesis in cotyledons of *Cucurbita pepo*. *Biochim Biophys Acta* 524(1):1–11
- Leegood RC, Walker RP (2003) Regulation and roles of phosphoenolpyruvate carboxykinase in plants. *Arch Biochem Biophys* 414(2):204–210
- Li TQ, Liu XF, Wan YM, Li ZH, Qi GH, Li YY, Liu XX, He R, Ma Y, Ma H (2017) Transcriptome analysis for (plant species with extremely small populations) based on high throughput sequencing. *Bull Bot Res* 37(6):825–834
- Liu KY, Ba XL, Yu JZ, Li J, Wei KQ, Han GD, Li GP, Cui Y (2006) The phosphoenolpyruvate carboxykinase of mycobacterium tuberculosis, induces strong cell-mediated immune responses in mice. *Mol Cell Biochem* 288(1–2):65–71
- Maciaga M, Paszkowski A (2004) Genetic control of aspartate aminotransferase isoenzymes in *Aegilops* and *Triticum* species. *J Appl Genet* 45(4):411–417
- Majumdar R, Minocha R, Minocha SC, D'Mello JPF (2015) Ornithine: at the crossroads of multiple paths to amino acids and polyamines. CAB International, pp 156–172
- Manzoor H, Kelloniemi J, Chiltz A, Wendehenne D, Alain P, Poinssot B, Garcia-Brugger A (2013) Involvement of the glutamate receptor *atglr3.3* in plant defense signaling and resistance to hyaloperonospora arabidopsidis. *Plant J* 76(3):466–480
- Martín M, Rius SP, Podestá FE (2011) Two phosphoenolpyruvate carboxykinases coexist in the crassulacean acid metabolism plant *Ananas comosus*. Isolation and characterization of the smaller 65 kDa form. *Plant Physiol Biochem* 49(6):646–653
- Mattoo AK, Fatima T, Upadhyay RK, Handa AK (2015) Polyamines in plants: biosynthesis from arginine, and metabolic, physiological and stress-response roles. In: D'Mello JPF (ed) *Amino acids in higher plants*. CAB International, Wallingford, pp 177–194
- Meijer AJ, Lamers WH, Chamuleau RA (1990) Nitrogen metabolism and ornithine cycle function. *Physiol Rev* 70(3):701–748
- Movahedi A, Zhang J, Amirian R, Zhuge Q (2014) An efficient agrobacterium-mediated transformation system for poplar. *Int J Mol Sci* 15(6):10780–10793
- Murooka Y, Mori Y, Hayashi M (2002) Variation of the amino acid content of *Arabidopsis* seeds by expressing soybean aspartate aminotransferase gene. *J Biosci Bioeng* 94(3):225–230
- Nakagawa T, Kurose T, Hino T, Tanaka K, Kawamukai M, Niwa Y, Toyooka K, Matsuoka K, Jinbo T, Kimura T (2007) Development of series of gateway binary vectors, pGWBs, for realizing efficient construction of fusion genes for plant transformation. *J Biosci Bioeng* 104(1):34–41
- Osorio S, Vallarino JG, Szczowka M, Ufaz S, Tzin V, Angelovici R, Gad G, Fernie RA (2013) Alteration of the interconversion of pyruvate and malate in the plastid or cytosol of ripening tomato fruit invokes diverse consequences on sugar but similar effects on



- cellular organic acid, metabolism, and transitory starch accumulation. *Plant Physiol* 161(2):628–643
- Owen OE, Kalhan SC, Hanson RW (2002) The key role of anaplerosis and cataplerosis for citric acid cycle function. *J Biol Chem* 277(34):30409–30412
- Pilot G, Stransky H, Bushey DF, Pratelli R, Ludewig U, Wingate VP, Frommer WB (2004) Overexpression of glutamine dumper1 leads to hypersecretion of glutamine from hydathodes of arabidopsis leaves. *Plant Cell* 16(7):1827–1840
- Pinto H, Sharwood RE, Tissue DT, Ghannoum O (2014) Photosynthesis of C<sub>3</sub>, C<sub>3</sub>–C<sub>4</sub>, and C<sub>4</sub> grasses at glacial CO<sub>2</sub>. *J Exp Bot* 65(13):3669–3681
- Price MB, Kong D, Okumoto S (2013) Inter-subunit interactions between glutamate-like receptors in Arabidopsis. *Plant Signal Behav* 8(12):e27034
- Roosens NH, Bitar FA, Loenders K, Angenon G, Jacobs M (2002) Overexpression of ornithine-δ-aminotransferase increases proline biosynthesis and confers osmotolerance in transgenic plants. *Mol Breeding* 9(2):73–80
- Shi JH, Yi KK, Yu L, Li X, Zhou ZJ, Chen Y, Hu ZH, Tao Z, Liu RH, Chen YL, Chen JQ (2015) Phosphoenolpyruvate carboxylase in Arabidopsis leaves plays a crucial role in carbon and nitrogen metabolism. *Plant Physiol* 167(3):671–681
- Sun Su (2018) Functional analysis of photosynthesis by transgenic maize *ZmPCK1* gene. *Jilin Agric Univ* 1(1):11–13
- Urbina JA, Osorno CE, Rojas A (1990) Inhibition of phosphoenolpyruvate carboxykinase from *Trypanosoma* (*Schizotrypanum*) cruzi epimastigotes by 3-mercaptopicolinic acid: in vitro and in vivo studies. *Arch Biochem Biophys* 282(1):91–99
- Walker RP, Chen ZH (2002) Phosphoenolpyruvate carboxykinase: structure, function and regulation. *Adv Bot Res* 38(02):93–189
- Walker RP, Leegood R (1996) Phosphorylation of phosphoenolpyruvate carboxykinase in plants. Studies in plants with C<sub>4</sub> photosynthesis and Crassulacean acid metabolism and in germinating seeds. *Biochem J* 317(3):653–658
- Walker R, Tecsí L, Famiani FP, Leegood R, Chen Z (1999) Phosphoenolpyruvate carboxykinase plays a role in interactions of carbon and nitrogen metabolism during grape seed development. *Planta* 210(1):9–18
- Walker RP, Benincasa P, Battistelli A, Moscatello S, Tecsí L, Leegood RC, Famiani F (2018) Gluconeogenesis and nitrogen metabolism in maize. *Plant Physiol Biochem* 130:324–333
- Wang JY (2011) Amino acid metabolism. *Biochemistry* 31:340–341
- Wang LN, Wang YC, Yang CP (2017) The comparative study of callus and direct differentiation regeneration system of 84K poplar. *Bull Bot Res* 37(4):542–548
- Wingler A (1999) Phosphoenolpyruvate carboxykinase is involved in the decarboxylation of aspartate in the bundle sheath of maize. *Plant Physiol* 120(2):539–546
- Yu ZH (2012) Research and application of HPCE-TOF/MS technology in the analysis of common toxic alkaloids. Doctoral dissertation, Fudan University, pp 8–11
- Zeng J, Kuang H, Hu C, Shi X, Yan M, Xu L, Xu GW (2013) Effect of bisphenol a on rat metabolic profiling studied by using capillary electrophoresis time-of-flight mass spectrometry. *Environ Sci Technol* 47(13):7457–7465
- Zhao JX (2016) A new method based on CE-MS for metabolomics analysis and its application in tobacco research. Doctoral dissertation, Dalian University of Technology, pp 43–45

**Publisher's Note** Springer Nature remains neutral with regard to jurisdictional claims in published maps and institutional affiliations.